AIP | The Journal of Chemical Physics

Proton transport in ice at 30–140 K: Effects of porosity

Caixia Bu and Raúl A. Baragiola

Citation: The Journal of Chemical Physics **143**, 074702 (2015); doi: 10.1063/1.4928506
View online: http://dx.doi.org/10.1063/1.4928506
View Table of Contents: http://scitation.aip.org/content/aip/journal/jcp/143/7?ver=pdfcov
Published by the AIP Publishing

Proton transport in ice at 30–140 K: Effects of porosity

Caixia Bu[a] and Raúl A. Baragiola[b]
Laboratory for Astrophysics and Surface Physics, Department of Materials Science and Engineering, University of Virginia, Charlottesville, Virginia 22904, USA

(Received 29 June 2015; accepted 30 July 2015; published online 18 August 2015)

We examined the role of porosity, a crucial characteristic of amorphous solid water (ASW), on electrostatic charging and discharging of ASW films with 500 eV He^+ and Xe^+ ions, by measuring the surface potentials with a Kelvin probe. When a charged ASW film is heated, its surface potential decreases sharply, at temperatures that depend on the maximum temperature the film was once subject to. This sharp decrease of the surface potential is not due to a large thermally induced increase of the dielectric constant ε as proposed in other studies, since measurements of ε yielded a value of ∼3 below ∼100 K. Rather, the potential drop can be explained by the transport of the surface charge to the substrate, which depends on film porosity. We propose that the charge migrates along the walls of the pores within the ASW film, facilitated by the thermally induced reorientation of the incompletely coordinated molecules on the pore walls. © *2015 AIP Publishing LLC*. [http://dx.doi.org/10.1063/1.4928506]

I. INTRODUCTION

Amorphous solid water (ASW), grown by condensation of water vapor onto cold surfaces (below ∼130 K), is the most common form of water in the universe. Research on ASW is driven by the desire to understand its properties in astrophysical environments such as interstellar dark clouds and the outer solar system.[1] A fundamental topic, studied for decades and still controversial, is the motion of ions in water ice at temperatures lower than 130 K. At higher temperatures, in the domain of crystalline ice (CI), proton mobility is theoretically expected to result from the Grotthuss mechanism in which protons tunnel across the hydrogen bond network of water molecules with very small activation energy.[2] A requirement for this mechanism is that molecules along the path of a proton rotate through the migration of orientational defects. In crystalline ice, water molecules are oriented such that there is a hydrogen atom between two oxygen atoms; the orientational defects are the sites where molecules are incorrectly oriented, either with no hydrogen atoms (L Bjerrum defects) or two hydrogen atoms (D Bjerrum defects) between two oxygen atoms.[2] Experiments with polycrystalline ice films suggest that proton motion is thermally activated, but the reports of the temperature range where transport is observable are inconsistent: above 120 K obtained indirectly by monitoring isotopic exchange in the bulk using IR spectroscopy,[3] above 190 K from the observed immobility of hydronium (H_3O^+) deposited on the surface using a Kelvin probe,[4] and above 95 K when surface charges were measured by reactive ion-surface scattering (RIS).[5] The reason for the high temperatures determined with H_3O^+ deposited on the surface[6] is that charges deposited on the surface self-trap, thus behaving differently than in the bulk, both in CI[7] and in ASW.[8] Our results using ions implanted at 500 eV and a Kelvin probe in CI are in agreement with the RIS data, while in ASW the temperature for charge mobility is lower and depends on the thermal history of the ice.

In earlier studies,[3–8] the nanoscale porosity, a crucial characteristic of ASW, was not taken into account explicitly. ASW presents a large internal surface area (up to hundreds of m^2/g),[9] due to pores ∼1 nm wide.[10,11] Experimental results have confirmed that the porosity of ASW decreases with increasing growth temperature and increases with increasing incidence angle of the vapor flux.[12,13] The porosity can be decreased after growth by thermal annealing[10,11] or by irradiation with fast ions.[14] To study possible effects of the microporous structure on ion migration, we prepared ASW films of various porosities and charged them by irradiation with 500 eV He^+ or Xe^+ ions. We used a Kelvin probe to measure the surface potential of the charged films with respect to the electrically grounded metal substrate and investigated the dependences of this potential on deposited charge, incidence angle of the vapor flux, and subsequent annealing at temperatures that increased linearly with time.

II. EXPERIMENTAL DETAILS

All experiments were conducted in an ultra-high vacuum system with a base pressure of $\sim 2 \times 10^{-10}$ Torr. ASW films were deposited from a collimated vapor beam[15] onto a gold-coated quartz crystal microbalance (QCM)[16] kept at temperatures below 130 K. The areal mass of the film, measured by the QCM, was used to deduce the column density (in units of monolayers, ML, defined as 1 ML = 10^{15} molecules/cm^2 or about 1 monolayer) by dividing by the molecular mass. The growth rate for all films was controlled at 0.2 ± 0.1 ML/s. The film thickness d was obtained by fitting the Fresnel equations to the interference pattern in the UV-visible optical reflectance[12] obtained with a FilmTek 2000 instrument (Scientific

[a]Author to whom correspondence should be addressed. Electronic mail: CaixiaBu@virginia.edu
[b]Deceased.

Computing International). The film density ρ was calculated from the ratio of the film areal mass to the thickness, and the porosity, $p = 1 - \rho/\rho_c$, was obtained using $\rho_c = 0.94$ g/cm^3 for the intrinsic density of compact ice.[17] The surface potential of the film with respect to the substrate was derived from the contact potential difference (CPD) measurements using a Kelvin probe (KP Technology Ltd., Model UHV KP 4.5).[18]

Irradiations were at normal incidence with a flux kept at $(0.4 \pm 0.1) \times 10^{10}$ ions/(cm^2 s), measured using a Faraday cup. The thickness of the films (~1100 ML) was in the range 0.3–0.5 μm, always much larger than the penetration depth of He^+ or Xe^+ ions at 500 eV [less than 0.02 μm based on Transport of Ions in Matter (TRIM)[19] simulations] and even larger than the projectile neutralization distance of about 0.0003 μm.[20]

When ions deposit a charge Q on top of a very thin surface layer of an insulator film condensed on an electrically grounded metal substrate, a surface potential (V_s) is created, given by

$$V_s = \frac{Qd}{A\varepsilon\varepsilon_o}, \tag{1}$$

where A is the irradiated area, d the film thickness, ε the dielectric constant of the film, and $\varepsilon_o = 8.854 \times 10^{-14}$ C/(V cm) the permittivity of vacuum. For ASW films annealed at 120 K, the linear dependence of V_s on d at 100 K was demonstrated previously using 55 eV Ar^+ incident ions.[21] Dielectric breakdown, observed for fast ion irradiation of thick films,[22] is absent under low energy ion impacts.

III. RESULTS AND DISCUSSION

A. Dielectric constant at 30 K

ASW films deposited at low temperatures (below 110 K) show negative surface potentials (V_s) because of spontaneous polarization during growth.[18,23,24] We first studied how this initial negative potential evolves as positive charge accumulates on the surface of the film. For this purpose, we condensed an ASW film (1108 ML) at 30 K with the vapor flux at normal incidence; the film showed a polarization-induced V_s of -13.8 ± 0.4 V. We then irradiated this film with 500 eV He^+ ions in 30-s intervals and measured the V_s after each interval. The surface potentials V_s are shown in Fig. 1 as a function of the accumulated fluence F, the integral of the ion flux over the irradiation time. The slope $\Delta V_s/\Delta F$ changes within the first few intervals but approaches a constant after the surface of the film becomes positive.

To explain the observations in Fig. 1, we assume that the electric fields due to spontaneous polarization and electrostatic charging are independent and additive; we will return to this assumption below. We use now a picture of the charging process for low energy ions, which differs from that used for deeply penetrating ions.[14,22] Low energy ions neutralize at the surface, resulting in positive holes (ions) in the solid.[20,21] Since the ionization energies for Xe and He (12.15 and 24.5 eV, respectively)[25] are greater than the ionization threshold for ice (~11 eV),[26] the formation of hydronium is energetically favorable as[21,27] $X^+ + (H_2O)_n \rightarrow X + (H_2O)^+_n$ (where X represents the incident ion), providing excess protons within the penetration depth (<20 nm). Effects of backscattered ions and sputtered ions are negligible in our experiments. Secondary electrons are ejected by different mechanisms;[22] their energy is limited to a few eV due to the large gap (~11 eV)[26] between the top of the valence band and the vacuum level of ASW. If the secondary electrons escape into vacuum, additional holes would result in the solid, near its surface (the electron escape depth is a few nm). Thus, the charge deposited is limited to a very thin surface layer, and the magnitude of the surface charge density is $Q/A = F(1 + \gamma')$, where γ' is smaller than the electron yield γ if the emitted electrons can return to the surface. At low fluence, the surface is negative because of the spontaneous polarization during growth, and thus, the electrons leave the surface, and $Q/A > F$. When the charge build-up produces a positive surface potential of several volts, most of the emitted secondary electrons (whose typical energies are a few eV) return back to the film, making $\gamma' = 0$. In this case, the growth rate of the deposited charge is determined by the ion flux, assuming leakage of charge to the substrate is insignificant; thus, the surface potential of the film increases linearly at higher fluence, following Eq. (1) with $Q/A = F$. From the ratio of the $\Delta V_s/\Delta F$ of the negative region of the V_s (F) graph to that of the positive region, $(1 + \gamma)/1$, we derive an electron yield $\gamma = 1.8 \pm 0.1$.

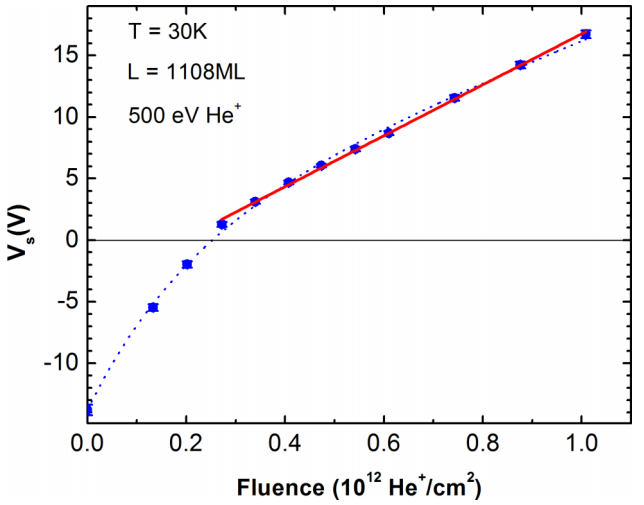

FIG. 1. Evolution of the surface potential of an ASW film (1108 ML, deposited at 30 K) with the accumulated ion fluence at 30 K. The solid-line is a straight-line fit to the positive data points, and the calculated dielectric constant ε with the fitting slope is 3.4 ± 0.5. The dotted line is to guide the eye.

We derive the dielectric constant ε from the slope ($k = d/\varepsilon\varepsilon_o = 1.29 \times 10^4$ V m^2 C^{-1}) of a straight-line fit to the positive data in Fig. 1. The thickness of the film obtained with the UV-visible interferometry is $d = (0.39 \pm 0.02)$ μm; therefore, the calculated dielectric constant is $\varepsilon = 3.4 \pm 0.5$. Another method to estimate the ε is by correcting the high-frequency dielectric constant of compact ice ε_c for porosity p using the Clausius–Mossotti (CM) equation $(\varepsilon_p - 1)/(\varepsilon_p + 2) = (1 - p)(\varepsilon_c - 1)/(\varepsilon_c + 2)$.[28,29] We use $\varepsilon_c = 3.2$, appropriate in the low temperature limit where molecules cannot rotate,[2] and the measured $p = 0.087$; thus, ε_p is 2.9. The calculated dielectric constant (~3.4) agrees with the value of 2.9 derived from the CM equation within errors (~15%).

B. Evolution of the surface potential with annealing temperature

In this section, we present results for the evolution of surface potential V_s with temperature (heating at a constant rate of 4.8 K/min, unless specified otherwise) and provide a model incorporating microporosity to explain our observations.

1. Effect of irradiation fluence

We return to the question of separability of the fields due to the initial polarization and the applied electrostatic charging by studying the dependence of surface potential on annealing temperature. Studies showed that ASW films depolarize when warmed, that is, the magnitude of the initial negative surface potential decreases.[18,24] Similarly, in the charging experiments, the ion-induced positive surface potential will also decrease, if the deposited surface charge migrates to the substrate or the dielectric constant increases while heating, cf. Eq. (1). In experiments to compare the thermal-induced decreases of these two voltages, three 1100-ML ASW films (***a***,***b***, and ***c***) were deposited at 30 K, showing polarization-induced V_s of -13.7 ± 0.4 V. Film ***a*** remained non-irradiated, film ***b*** was charged to -3.2 ± 0.2 V at 30 K by 0.2×10^{12} He^+/cm^2, and film ***c*** was charged to $+18.7 \pm 0.4$ V by 1.1×10^{12} He^+/cm^2. The evolutions of V_s for the three films during heating are shown in Fig. 2(a).

If the fields due to the initial polarization and the applied electrostatic charging are independent and additive, we can express the surface potential (V_s) of a charged film as a combination of a negative polarization voltage (V_-) and a positive electrostatic charging voltage (V_+). At 30 K, V_- for the three curves in Fig. 2(a) is the same, −13.7 V; $V_+(\boldsymbol{b}) = -3.2 - (-13.7)$ V = 10.5 V, and $V_+(\boldsymbol{c}) = +18.7 - (-13.7)$ V = 32.4 V. Under the assumption that the thermal evolution of polarization is the same for the three films, the thermal decrease of V_+ is obtained by subtracting $V_s(\boldsymbol{a})$ from the $V_s(\boldsymbol{b})$ and $V_s(\boldsymbol{c})$; the results are shown in Fig. 2(b). The dashed line ***b*-*a*** in Fig. 2(b) is produced by $(10.5/32.4) \times V_+(\boldsymbol{c})$ and is indistinguishable from $V_+(\boldsymbol{b})$ (solid-line ***b*-*a***), suggesting that the thermal evolutions of the electrostatic charging V_+ of the films ***b*** and ***c*** can be normalized to the same curve. Thus, the polarization-induced negative surface potential and the ion-induced positive surface potential can be separated and evolve independently as temperature increases. The inset of Fig. 2(b) shows that the drop in magnitude of the positive surface potential is faster with temperature than that of the negative polarization voltage. The same results were obtained using 500 eV Xe^+ ions. This is consistent with the proposed mechanism that both He and Xe ions neutralize and produce an excess of protons on the surface of the films.

2. Charging of pre-annealed ASW films

To further investigate the thermal discharging of the films, we varied the polarization-induced fields in the films, rather than the ion-induced fields, by pre-annealing the films to different temperatures before ion irradiation. Four 1100-ML ASW films were deposited at 30 K at normal incidence, pre-annealed at T_a = 60, 80, 120, and 140 K, and then cooled back to 30 K, producing $V_s = -3.8 \pm 0.2$, -0.86 ± 0.09, -0.19 ± 0.09, and -0.09 ± 0.09 V, respectively. These pre-annealed films were charged at 30 K to similar surface potentials of 16.2, 15.9, 15.9, and 16.2 V, all ±0.3 V, using similar fluences. These charged films were then subject to heating from 30 K to 200 K. We note that these pre-annealed films showed different negative potentials ($|V_s| < 4$ V) before irradiations, which results in the escape of secondary electrons as discussed earlier, but this is only important for the T_a = 60 K curve. To correct for secondary electrons, we use $F' = k \times F$ with the factor k obtained being important only for the T_a = 60 K film, k = 1.1. A small (−3.6 V at F = 0) but significant contribution of intrinsic polarization in the T_a = 60 K curve was subtracted using data from our previous study,[18] obtained without ion irradiation. The ratio of surface potential to the corrected fluence is proportional to the ratio of the film

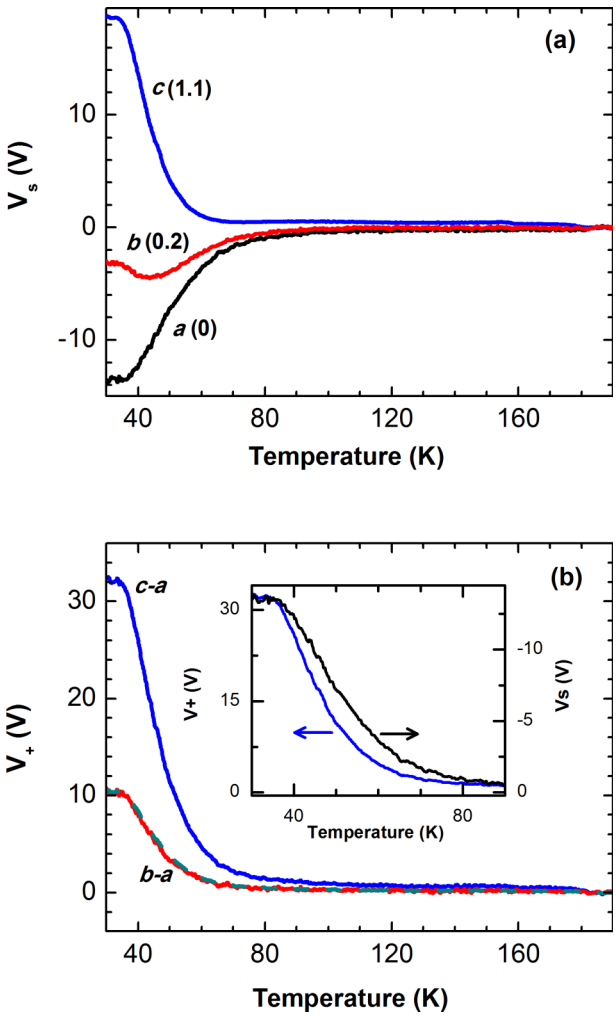

FIG. 2. (a) Evolution of the surface potential while heating films from 30 K at 4.8 K/min. Three 1100-ML ASW films were condensed at 30 K at normal incidence, showing surface potentials of $V_s = -13.7 \pm 0.4$ V; film ***a*** was not charged whereas the films ***b*** and ***c*** were charged at 30 K by the fluences of 500 eV He^+, indicated next to the curve labels (in units of 10^{12} He^+/cm^2). (b) Thermal evolution of the positive electrostatic voltages, derived from the top panel by subtracting curve ***a*** from the curves ***b*** and ***c***. The dashed line is produced by [(10.5/32.4)×line ***c*-*a***] (see text for the explanations of the numbers) and is indistinguishable from the solid-line ***b*-*a***. *Inset*: During heating, the positive voltage (right axis) decreases faster than the negative polarization voltage (left axis, note the inverted signs).

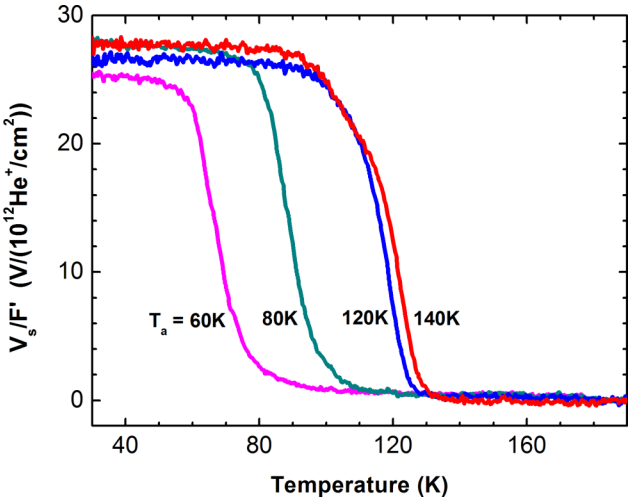

FIG. 3. Thermal evolutions of the ratios V_s/F' during heating of ASW films charged by 500 eV He^+. The ASW films were deposited at 30 K, pre-annealed at $T_a = 60$ K, 80 K, 120 K, and 140 K, and then cooled to 30 K. The films were charged to ~16 V at 30 K. The ratios V_s/F' (where F' is corrected for secondary electron emission) are similar in all the films before dropping sharply, showing that the dielectric constant does not depend strongly on the pre-heating treatment. The sharp drops of V_s/F', attributed to migration of deposited charge to the substrate, occur at temperatures greater than the pre-heating temperature T_a when T_a is below ~100 K and at ~100 K when $T_a = 120$ and 140 K. [Adapted with permission from C. Bu *et al.*, J. Chem. Phys. **142**, 134702 (2015). Copyright 2015 AIP Publishing LLC.].

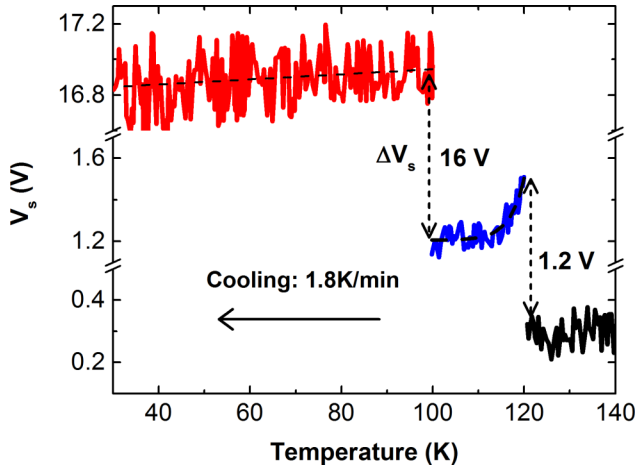

FIG. 4. Evolution of the surface potential during cooling of a charged film. A 1107-ML ice film, deposited at 30 K and annealed at 140 K, was successively charged at 140 K, 120 K, and 100 K with the same fluence of $(0.54 \pm 0.09) \times 10^{12}$ Xe^+/cm^2 at 500 eV. Dashed lines are to guide the eye.

thickness to the dielectric constant ($V_s/F' \propto d/\varepsilon$). Thus, to focus on the intrinsic parameter $1/\varepsilon$ during heating, we present the thermal evolutions of V_s/F' of the charged films in Fig. 3, rather than V_s. It shows that, with increasing temperature, the ratio V_s/F' of the four films stays roughly constant within the 15% experimental error and then decreases sharply when the temperature exceeds a value depending on the maximum temperature reached in the pre-annealing cycle.

Tsekouras *et al.*[6] reported similar data to that of Fig. 3 and interpreted the decrease of the surface potential with temperature as result from a large, irreversible increase of the dielectric constant ε when the films were heated above a temperature higher than previously attained in its thermal history. For instance, it was reported that the ε changes from ~2 at 30 K to a large value lying between 37 and 56 at 60 K and that the ε remains large upon subsequent cooling of the ice films.[6] If that interpretation were correct, ASW films annealed to higher T_a in the first annealing cycle would have larger values of ε and consequently smaller values of V_s/F'. Rather, Fig. 3 shows that V_s/F' is approximately constant below the annealing temperature for films with different T_a, indicating that the ε is roughly temperature-independent, given that reduction in d by thermal compaction during pre-annealing is less than 12%.[30] The dielectric constant, $\varepsilon = (d/\varepsilon_o)/(V_s/F')$, was calculated using the measured values of d, V_s, and F' in the plateau of each film. The average of these calculations is $\bar{\varepsilon} = 2.5 \pm 0.4$, agreeing within errors with 3.4 ± 0.5 calculated from Fig. 1. Given the temperature independence of the dielectric constant, the sharp decrease of V_s/F' by a few orders of magnitude at temperatures somewhat higher than the T_a (or ~100 K if T_a is above ~100 K) must be attributed to the migration of the deposited charge to the grounded substrate.

3. Dependence on thermal history

We pursued additional evidence for our proposed charge migration as an explanation of the voltage drops in Fig. 3. We deposited a 1107-ML ASW film at 30 K at normal incidence and heated it to 140 K, destroying all or most of the spontaneous polarization ($V_s = -0.09 \pm 0.09$ V). The film was subsequently irradiated at 140 K with 500 eV Xe^+ ions, cooled to 120 K, irradiated again, then cooled to 100 K, and irradiated for a third time; the fluence for each irradiation was the same, $(0.54 \pm 0.09) \times 10^{12}$ ions/cm^2. The film was finally cooled continuously to 30 K while recording the surface potential shown in Fig. 4.

If the deposited charge were immobile on the film from 30 to 190 K and the ε constant during cooling, as proposed by Tsekouras *et al.*,[6] we would expect the same ion-induced change of the surface potential ΔV_s at the three irradiation temperatures, since $\Delta V_s/\Delta Q = d/(A\varepsilon\varepsilon_o)$ and ΔQ were kept constant by keeping a constant fluence. However, ΔV_s, rather than being constant, is ~0.3, 1.2, and 16 V at 140, 120, and 100 K, respectively. Also, we observe a fast decay of V_s during cooling from 120 to 100 K but a relative constant V_s during cooling from 100 to 30 K. Both observations imply that ΔQ drops, i.e., the deposited charges migrate to the substrate at temperatures above ~100 K, rather than stay immobile on the surface of the film.

We do not observe the decay of V_s during cooling from 140 to 120 K, and it is likely that the charge migration rate at 140 K is so fast that the majority of the deposited charges have migrated to the substrate before we can start the measurements of V_s, as it takes ~60 s after the end of each irradiation to initiate these measurements. We interpret the small positive voltage (~0.3 V) after irradiation at 140 K as due to a small fraction of the charges trapped at defects.

4. Experiments with sandwiched ions

Recent experiments by Kang *et al.*[7,8] suggest that protons have the thermodynamic propensity to reside at the surface of

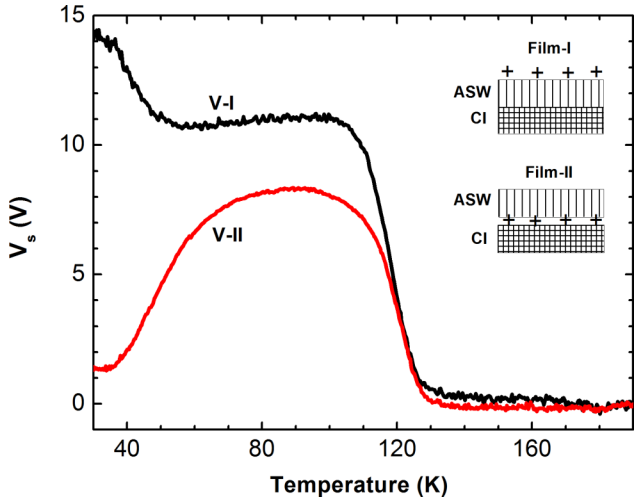

FIG. 5. Evolution of surface potentials while heating the double-layered films, consisting of an ASW layer (deposited at 30 K at normal incidence) atop a crystalline layer, both 510 ML. The same ion fluence, 0.5×10^{12} ions/cm^2, was deposited at 30 K atop the ASW layer in Film-I and at the interface of the two layers in Film-II.

water ice rather than in its interior; they migrate from a shallow embedded layer to the surface. Here, we designed experiments to examine the charge migration direction in ASW ice films. We prepared two double-layered films (510-ML each layer), consisting an ASW ice layer deposited at 30 K atop a CI layer (annealed at 140 K). Excess charges were introduced at 30 K on the vacuum-ASW interface of the first film by depositing 0.5×10^{12} Xe^+/cm^2 (energy = 500 eV) after the deposition of the ASW layer (Film-I in Fig. 5), while sandwiched at the ASW-CI interface of the second film by depositing the same ion fluence but prior to the deposition of the ASW layer (Film-II in Fig. 5). Afterward, both films were heated from 30 to 200 K.

At 30 K, in the first case, the surface potential of just the CI layer was -0.02 ± 0.01 V as prepared, -6.6 ± 0.2 V after the deposition of the ASW overlayer, and 14.5 ± 0.3 V with the charge deposited on top. In the second case, the surface potential of just the CI layer was also -0.02 ± 0.01 V, 8.2 ± 0.2 V after charging, and decreased to 1.5 ± 0.1 V after the deposition of the ASW overlayer. Note that the polarization voltage of the ASW layer of Film-II is -6.7 ± 0.2 V, the same within errors as that of the ASW layer of Film-I.

Upon heating, the surface potential of Film-I (curve V-I in Fig. 5) decreases sharply at ~35 K, reaches a plateau between ~50 and 90 K, and decreases sharply again at ~100 K. We learned from Fig. 2 (curve **c**) and Fig. 3 (curve T_a = 140 K) that most of the deposited charge has migrated through the ASW film at ~70 K but stays atop the CI film until ~100 K. Thus, in Film-I, we expect that the charge first migrates through the ASW layer below ~70 K and then stays at the ASW-CI interface until temperatures exceed ~100 K. The plateau level at ~11 V is consistent with the near disappearance of the spontaneous polarization [Fig. 2(a)] and the reduction of the potential due to ion charging (14.5 + 6.6 = 21.1 V) as the charges migrate to the ASW-CI interface, about halfway in the film. The existence of the plateau indicates that the charges stay at the interface and do not migrate through the CI film until about 100 K.

The thermal evolution of V_s of Film-II has a bell shape: it increases sharply at ~35 K as the negative polarization fades, reaches a maximum of 8.3 V at ~90 K, and then decreases abruptly at ~95 K. The maximum of 8.3 V is consistent with the charging potential of 8.2 V obtained prior to the deposition of the top ASW layer. The potential then decreases similarly to that of Film-I as the charge migrates to the substrate. Our observations in Fig. 5 show no evidence supporting the migration of charge from the interior to the film-vacuum interface.

5. Dependence on deposition angle

Seeking a mechanism that enables charge migration through the ASW films, we examine now the effect of porosity. This is a salient feature of ASW that affects many properties, such as spontaneous polarization[18] and infrared absorption,[3] but has been rarely discussed in the context of charge activity in ice.[2] The porosity of ASW increases greatly with increasing incidence angle of the vapor flux;[10,13] thus, to vary the porosity of 1100-ML ASW films at 30 K, we used different incidence angles of 0°, 20°, 45°, and 70° of the incident vapor flux. These films were then irradiated at 30 K with the same fluence of 500 eV He^+ ions, 10^{12} He^+/cm^2, and then heated to 200 K. For the same amount of surface charge, the surface potential V_s increases linearly with film thickness d (Eq. (1)) but the internal electric field ($E = V_s/d$) stays constant. Thus, to avoid this thickness effect, we look at the electric fields; Fig. 6 shows the thermal evolutions of the electric fields, and the inset the evolutions scaled at 30 K. One notices that, though in all cases the field E decreases with annealing temperature, the decrease is remarkably smaller for the film deposited at 70° (~84% at 60 K) than for films deposited at smaller angles (~93% at 60 K). The distinct behavior in the film grown at 70° incidence is likely related to the wider mesopores produced only at large deposition angles,[10] which collapse more gradually than nanopores, suggesting that the particular porous structure plays a role in the electrostatic discharging of the ASW films during heating.

C. Discussion: The role of porosity

Proton activity in crystalline water ice has been studied for decades, as discussed above. Quantitative infrared studies showed conclusively that protons migrate within *crystalline* or *polycrystalline* water ice at temperatures as low as 130 K in accord with the Grotthuss mechanism, in which the proton activity is mainly determined by the concentration and mobility of both the excess protons and orientational defects.[2,31] Reports on proton activity in ASW are much sparser.[7,32] An interesting conclusion derived from recent investigations on ASW films (a few monolayers thick) is that the proton activity at 90–140 K at the surface is at least an order of magnitude greater than in the interior, consistent with results of isotopic exchange using nanocrystals,[33] and it is attributed to the presence of dangling bonds and disordered arrangement of molecules on the surface (referred as external surface).[7,8]

ASW at low temperatures has a microporous structure and thereby large internal surfaces (hundreds of m^2/g).[9]

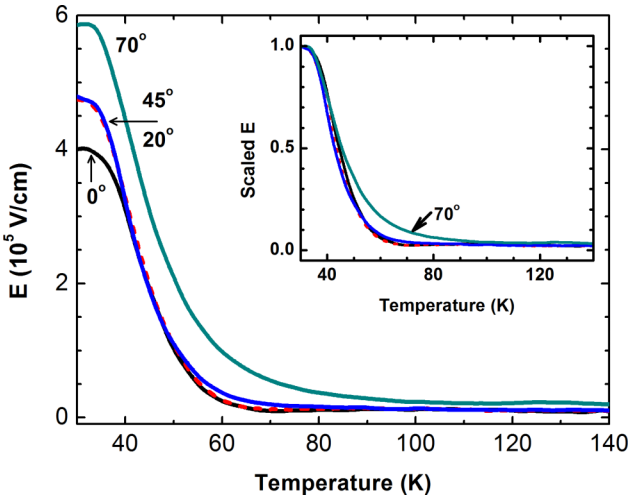

FIG. 6. Thermal evolution of the internal electric fields ($E = V_s/d$) during heating charged films of various porosities. The 1100-ML films were deposited at 30 K at 0°, 20°, 45°, and 70° incidence and irradiated at 30 K with the same fluence prior to heating. The inset with normalized values helps visualize the distinct behavior of the film deposited at 70°.

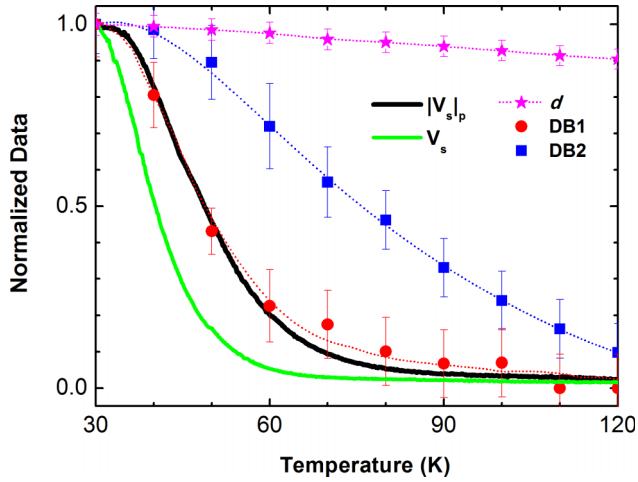

FIG. 7. Thermal evolutions of the surface potential V_s and the thickness d of an ASW film charged by 10^{12} He^+/cm^2 at 500 eV. Also shown are thermal evolutions of the magnitude of the polarization voltage $|V_s|_p$ and the integrated infrared absorbance of DB1 and DB2 bands. Data were normalized to values at 30 K, and the integrated absorbance of the DB1 and DB2 bands were calculated after subtractions of the continuum baseline absorption. [Adapted with permission from C. Bu *et al.*, J. Chem. Phys. **142**, 134702 (2015). Copyright 2015 AIP Publishing LLC.]

Incompletely coordinated water molecules, negligible in crystalline ice, are abundant on the internal surfaces, indicated by the enhanced infrared absorption features for dangling O–H bonds (DBs) around 3720 cm^{-1} and 3696 cm^{-1} (DB1 and DB2, assigned to O–H vibration of two- and three-coordinated molecules, respectively).[34,35] At temperatures below ~100 K in ASW, the mobility of possible orientational defects and/or the rotation of the tetrahedrally bonded water molecules are limited;[2,32] thus, the required molecular rotation for the migration of protons is unlikely satisfied via the same mechanism as that in the crystalline ice. Rather, led by the observed correlations between charge migration and porosity in the ASW films in Fig. 6, we suggest that incompletely coordinated molecules, flexible to undergo thermal-induced rearrangement at low temperatures,[10,11] are active in proton migration in ASW. We propose that, resembling observations on the external surface,[7,8] the proton activity is high also on the internal surface areas. The charge deposited on the ASW films tends to migrate to the metal substrate under the electric field induced by the charge and its image; once heated, the thermal energy activates the proton tunneling along hydrogen bonds between adjacent molecules due to the low activation energy,[31,36] and the subsequent rotation of water molecules is achieved via the thermal-induced rearrangement of the incompletely coordinated surface molecules.[34,35] Unlike other models,[36] this proposed mechanism allows the long-range vertical and interlayer charge migration along the walls of the pores in ASW films, since most of the pores are connected to the external surface.[10] In the bulk, water molecules are four-coordinated, and rotation of these molecules requires breaking the hydrogen bonds, which is unlikely at low temperatures. Above ~100 K, activated defects, bulk diffusion, and crystallization change the nature of the problem.[2,32]

To test our proposed mechanism, we monitor the thermal-induced rearrangement of the incompletely coordinated surface molecules by the integrated infrared absorbance of the DB1 and DB2[18] and compare their evolutions with those of the surface potentials of the ASW films, shown in Fig. 7. The magnitude of the polarization voltage $|V_s|_p$ of the intrinsic ASW film and the surface potential V_s of the charged ASW film share similar trends with the DBs, especially DB1, supporting that the incompletely coordinated molecules are essential for the electrical properties of the ASW films. As discussed in our earlier study,[18] the polarization results from alignment of incompletely coordinated molecules. In the charging experiments here, the projectile ions have very shallow penetrations, and a large fraction of the incompletely coordinated molecules, including their alignments, should not be affected by the deposited charge, consistent with our assumption that the polarization-induced and ion-induced voltages are independent and additive. The thermally induced rearrangement of the incompletely coordinated molecules, indicated by the decreases of the DBs in Fig. 7, is irreversible when cooling back the films,[34] consistent with the observed T_a-dependence of the surface potential in Fig. 3. At the same heating rate, we notice in Fig. 7 that V_s decreases faster than the $|V_s|_p$ and DB1.

Effects of the rearrangements of incompletely coordinated water molecules in ASW, already noticeable at constant temperature,[37–39] are evident in the isothermal relaxation of the surface potential V_s for charged ASW vs. CI films. Two 1110-ML ASW films were deposited at 30 K at normal incidence, showing polarization voltages of -13.8 ± 0.4 V; one of the films was crystallized by annealing at 140 K, removing any polarization and porosity, then cooled back down to 30 K. Both the ASW and CI films were then irradiated at 30 K to comparable surface potentials (16.7 V and 19.5 V, respectively), heated to 37 K at 1.8 K/min, and then held at 37 K for 800 s. Figure 8 shows that, for porous ASW, the V_s decreases slowly with time at 37 K, as well as during heating from 30 to 37 K (inset of Fig. 8), but stays constant for the crystalline film.

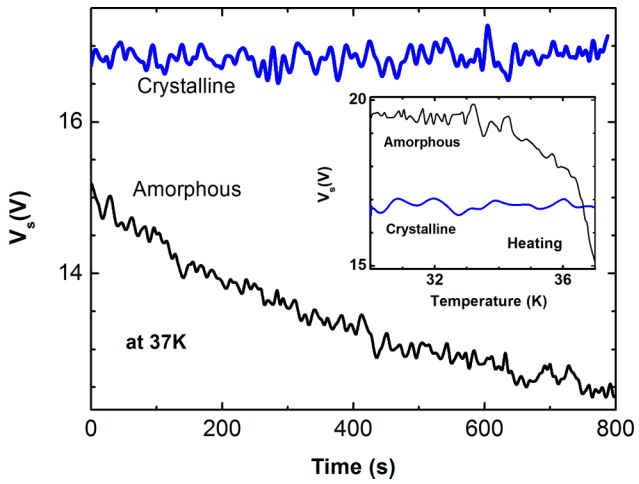

FIG. 8. Comparisons of the surface potential relaxations at 37 K of charged 1110-ML ASW (grown at 30 K) and crystalline (annealed at 140 K) ice films. Both films were charged at 30 K and then heated to 37 K at 1.8 K/min. Inset: Evolution of the surface potentials during heating from 30 to 37 K.

IV. SUMMARY AND CONCLUSIONS

We have examined the ion transport in water ice in the range of 30–140 K by depositing charges to the films via 500 eV ions and monitoring the surface potentials using a Kelvin probe. We derived a dielectric constant of ≈3 between 30 and 95 K. In experiments using ASW films deposited at 30 K under similar conditions but charged to different fluences at 30 K, our measurements show that the electric fields due to spontaneous polarization and electrostatic charging can be separated; they evolve independently as temperature increases, with a faster rate for the latter. Upon heating the charged ice films pre-annealed at different temperatures, we observed sharp decreases of the surface potentials at temperatures that strongly depend on the pre-annealing temperatures. Rather than a drastic increase of the dielectric constant claimed previously, we attribute the thermally induced decrease of the surface potentials at low temperatures (below ~100 K) to the migration of the deposited charge through the film to the substrate. The observed correlations between the thermal evolution of the surface potential and porosity suggest a role of the porous structure in the electrostatic discharging of the ASW films. We thus propose that the thermal-induced leakage of the deposited charge occurs along the walls of the pores at temperatures below ~100 K, facilitated by the thermal-induced rearrangement of the incompletely coordinated surface molecules. This proposed mechanism, supported by our infrared spectroscopic measurements, points to the role of porosity, a salient feature of ASW, in charge activity in ASW and explains the surface potential measurements consistently.

ACKNOWLEDGMENTS

During the review of this work, co-author Raúl Baragiola unexpectedly passed away. Without Raúl's encouragement and oversight, this work would not have been completed—his thoughts and contributions were invaluable, as well as our many office and home discussions.

This work was supported by NASA's Outer Planets Research Program. The authors thank U. Raut and E. Mitchell for many helpful discussions and sharing their infrared data and thank C. Dukes for edits and comments on the manuscript.

[1]R. A. Baragiola, Planet Space Sci. **51**, 953 (2003).
[2]P. V. Hobbs, *Ice Physics* (Clarendon, Oxford, 1974).
[3]P. J. Wooldridge and J. P. Devlin, J. Chem. Phys. **88**, 3086 (1988).
[4]J. P. Cowin, A. A. Tsekouras, M. J. Iedema, K. Wu, and G. B. Ellison, Nature **398**, 405 (1999).
[5]S. C. Park, K. H. Jung, and H. Kang, J. Chem. Phys. **121**, 2765 (2004).
[6]A. A. Tsekouras, M. J. Iedema, and J. P. Cowin, Phys. Rev. Lett. **80**, 26 (1998).
[7]C. W. Lee, P. R. Lee, and H. Kang, Angew. Chem., Int. Ed. **45**, 5529 (2006).
[8]E. S. Moon, C. W. Lee, and H. Kang, Phys. Chem. Chem. Phys. **10**, 4814 (2008).
[9]E. Mayer and R. Pletzer, Nature (London) **319**, 298 (1986).
[10]U. Raut, M. Fama, B. D. Teolis, and R. A. Baragiola, J. Chem. Phys. **127**, 204713 (2007).
[11]C. Mitterdorfer, M. Bauer, T. G. A. Youngs, D. T. Bowron, C. R. Hill, H. J. Fraser, J. L. Finney, and T. Loerting, Phys. Chem. Chem. Phys. **16**, 16013 (2014).
[12]M. S. Westley, G. A. Baratta, and R. A. Baragiola, J. Chem. Phys. **108**, 8 (1998).
[13]K. P. Stevenson, G. A. Kimmel, Z. Dohnalek, R. S. Smith, and B. D. Kay, Science **283**, 1505 (1999).
[14]U. Raut, B. D. Teolis, M. J. Loeffler, R. A. Vidal, M. Fama, and R. A. Baragiola, J. Chem. Phys. **126**, 244511 (2007).
[15]N. J. Sack and R. A. Baragiola, Phys. Rev. B **48**, 9973 (1993).
[16]M. A. Allodi *et al.*, Space Sci. Rev. **180**, 101 (2013).
[17]A. H. Narten, C. G. Venkatesh, and S. A. Rice, J. Chem. Phys. **64**, 1106 (1976).
[18]C. Bu, J. Shi, U. Raut, E. H. Mitchell, and R. A. Baragiola, J. Chem. Phys. **142**, 134702 (2015).
[19]J. F. Ziegler and J. P. Biersack, SRIM 2003, Stopping and Range of Ions in Matter, 2006, available at www.srim.org.
[20]R. A. Baragiola, in *Low Energy Ion-Surface Interactions*, edited by J. W. Rabalais (Wiley, New York, 1994), Chap. 4.
[21]Y. Horowitz and M. Asscher, J. Chem. Phys. **136**, 134701 (2012).
[22]J. Shi, M. Fama, B. D. Teolis, and R. A. Baragiola, Nucl. Instrum. Methods Phys. Res., Sect. B **268**, 2888 (2010).
[23]K. Kutzner, Thin Solid Films **14**, 49 (1972).
[24]M. J. Iedema, M. J. Dresser, D. L. Doering, J. B. Rowland, W. P. Hess, A. A. Teskouras, and J. P. Cowin, J. Phys. Chem. B **102**, 9203 (1998).
[25]*CRC Handbook of Chemistry and Physics*, 85th ed., edited by D. R. Lide (CRC Press, Boca Raton, FL, 2004).
[26]B. Baron and F. Williams, J. Chem. Phys. **64**, 3896 (1976).
[27]M. Akbulut, T. E. Madey, and P. Nordlander, J. Chem. Phys. **106**, 2801 (1997).
[28]D. E. Aspnes, Thin Solid Films **89**, 249 (1982).
[29]K. Maex *et al.*, J. Appl. Phys. **93**, 8793 (2003).
[30]J. B. Bossa, K. Isokoski, M. S. de Valois, and H. Linnartz, Astron. Astrophys. **545**, A82 (2012).
[31]W. B. Collier, G. Ritzhaupt, and J. P. Devlin, J. Phys. Chem. **88**, 363 (1984).
[32]M. Fisher and J. P. Devlin, J. Phys. Chem. **99**, 11585 (1995).
[33]J. P. Devlin and V. Buch, J. Chem. Phys. **127**, 091101 (2007).
[34]B. Rowland and J. P. Devlin, J. Chem. Phys. **94**, 812 (1991).
[35]V. Buch and J. P. Devlin, J. Chem. Phys. **94**, 4091 (1991).
[36]E. S. Moon, J. Yoon, and H. Kang, J. Chem. Phys. **133**, 044709 (2010).
[37]B. Schmitt, J. Ocampo, and J. Klinger, J. Phys. Colloq. **48**, C1–519 (1987).
[38]J. Hessinger and R. O. Pohl, J. Non-Cryst. Solids **208**, 151–161 (1996).
[39]Y. C. Wu, J. Jiang, S. J. Wang, A. Kallis, and P. G. Coleman, Phys. Rev. B **84**, 064123 (2011).